Received: 27 November 2019 | Revised: 13 March 2020 | Accepted: 18 March 2020

DOI: 10.1111/cas.14394

ORIGINAL ARTICLE

Cancer Science WILEY

FNDC3B 3′-UTR shortening escapes from microRNA-mediated gene repression and promotes nasopharyngeal carcinoma progression

Ying-Qing Li[1] | Yang Chen[1] | Ya-Fei Xu[2] | Qing-Mei He[1] | Xiao-Jing Yang[1] | Ying-Qin Li[1] | Xiao-Hong Hong[1] | Sheng-Yan Huang[1] | Ling-Long Tang[1] | Na Liu[1]

[1]State Key Laboratory of Oncology in South China; Collaborative Innovation Center of Cancer Medicine; Guangdong Key Laboratory of Nasopharyngeal Carcinoma Diagnosis and Therapy; Sun Yat-sen University Cancer Center, Guangzhou, China

[2]Department of Cell Biology and Genetics, Shenzhen University Health Science Center, Shenzhen, China

Correspondence
Na Liu and Ling-Long Tang, State Key Laboratory of Oncology in South China, Sun Yat-sen University Cancer Center, 651 Dongfeng Road East, Guangzhou 510060, China.
Emails: liun1@sysucc.org.cn (NL); tangll@sysucc.org.cn (LLT)

Funding information
Key-Area Research and Development Program of Guangdong Province, Grant/Award Number: 2019B020230002; National Natural Science Foundation of China, Grant/Award Number: 81572962 and 81802705; Natural Science Foundation of Guangdong Province, Grant/Award Number: 2017A030310468 and 2017A030312003; Health and Medical Collaborative Innovation Project of Guangzhou City, China, Grant/Award Number: 201803040003

Abstract

Alternative polyadenylation (APA), which induces shortening of the 3′-UTR, is emerging as an important feature in cancer development and progression. Nevertheless, the effects and mechanisms of APA-induced 3′-UTR shortening in nasopharyngeal carcinoma (NPC) remain largely unclear. Fibronectin type III domain containing 3B (*FNDC3B*) tended to use proximal polyadenylation site and produce shorter 3′-UTR according to our previous sequencing study. Herein, we found that *FNDC3B* with shorter 3′-UTR could escape from miRNA-mediated gene repression, and caused its increased expression in NPC. Knocking down of *FNDC3B* inhibited NPC cell proliferation, migration, invasion, and metastasis in vitro and in vivo. Overexpression of *FNDC3B*, especially those with shorter 3′-UTR, promoted NPC progression. Furthermore, the mechanism study revealed that *FNDC3B* could bind to and stabilize myosin heavy chain 9 (*MYH9*) to activate the Wnt/β-catenin signaling pathway. In addition, *MYH9* could reverse the inhibitory effects of *FNDC3B* knockdown in NPC. Altogether, our results suggested that the 3′-UTR shortening of *FNDC3B* mRNA mediated its overexpression in NPC and promoted NPC progression by targeting *MYH9*. This newly identified *FNDC3B*-*MYH9*-Wnt/β-catenin axis could represent potential targets for individualized treatment in NPC.

KEYWORDS

alternative polyadenylation, *FND3CB*, mRNA 3′-UTR shortening, nasopharyngeal carcinoma, proliferation and metastasis

1 | INTRODUCTION

Nasopharyngeal carcinoma (NPC), which arises from the epithelium of the nasopharynx, is one of the most common types of head and neck malignant tumor. Nasopharyngeal carcinoma is highly prevalent in South China, accounting for 47% of new cases worldwide.[1] Advances in the management, including the improvement of intensity-modulated radiotherapy and the broader application of

Li, Chen, and Xu contributed equally to this work.

chemotherapy, have dramatically improved overall survival of NPC patients.[2] However, the 5-year survival rate of NPC patients is still not satisfactory, due to local recurrence and distant metastasis in approximately 20% of patients.[3] Thus, to better understand the molecular mechanisms of NPC is still important for the development of novel therapeutic strategies.

As we know, 3′-end polyadenylation is a critical step of eukaryotic mRNA processing to maturation.[4] Alternative polyadenylation (APA) generates multiple mRNA isoforms, among which the shorter ones can escape from translation repression or mRNA degradation mediated by microRNAs (miRNAs) or other RNA regulatory elements within its 3′-UTRs.[5] Recently, shortening of mRNA 3′-UTRs has been reported to be involved in the pathogenesis and progression of certain malignancies.[6-8] The shortening of mRNA 3′-UTRs results in the activation of oncogenes and the repression of tumor suppressors.[9,10] It has been reported that 3′-UTR shortening of certain genes could enhance tumor cell proliferation, migration, and invasion.[11-13] In addition, shorter 3′-UTRs of target genes were associated with poor prognosis of certain tumors, such as breast, lung, colorectal, and bladder cancers.[13-15] Our previous high-throughput sequencing study showed that the APA phenomenon was prevalent in NPC, and several genes tended to use proximal polyadenylation site and produce shorter 3′-UTRs, such as fibronectin type III domain containing 3B (*FNDC3B*).[16] However, the functions and mechanisms of *FNDC3B* 3′-UTR shortening in NPC are not fully elucidated.

Herein, we found that *FND3CB* with shorter 3′-UTR could escape from miRNA-mediated gene repression, and caused its increased expression in NPC. Knockdown of *FNDC3B* could suppress NPC cell proliferation, migration, and invasion in vitro and in vivo. Overexpression of *FNDC3B*, especially its shorter 3′-UTR transcript, promoted NPC progression. The mechanism study revealed that *FND3CB* could stabilize myosin heavy chain 9 (*MYH9*) to stimulate the Wnt/β-catenin signaling pathway. Altogether, our results suggested that the 3′-UTR shortening of *FNDC3B* mediated its high expression in NPC and promoted NPC progression by targeting *MYH9*, thus providing potential therapeutic targets for NPC patients.

2 | MATERIALS AND METHODS

2.1 | Cell culture and clinical samples

All of the human immortalized nasopharyngeal epithelial cell NP69 and human NPC cell lines were generously provided by Professor Musheng Zeng (Sun Yat-sen University Cancer Center, Guangzhou, China). The NP69 was maintained in keratinocyte serum-free medium (Invitrogen) supplemented with bovine pituitary extract (BD Biosciences). The NPC cell lines (CNE-1, CNE-2, HONE-1, SUNE-1, HNE-1, 5-8F, and 6-10B) were cultured in RPMI-1640 (Invitrogen) supplemented with 5% FBS (Gibco). All of the cell lines were incubated at 37°C in a humidified atmosphere with 5% CO_2.

Twelve freshly frozen NPC and 8 normal nasopharynx tissues were collected from the Sun Yat-sen University Cancer Center. None of the patients had received antitumor therapy before sampling. Our studies were undertaken on the basis of the Declaration of Helsinki and approved by the Institutional Ethical Review Boards of Sun Yat-sen University Cancer Center. Written informed consent was obtained from all patients.

2.2 | Plasmid construction and transfection

The *FNDC3B* shRNA (#1: forward [F], 5′-CCGGGCAGCCCAAAGTCGAATGATTCTCGAGAATCATTCGACTTTGGGCTGCTTTTTG-3′ and reverse [R], 5′-AATTCAAAAAGCAGCCCAAAGTCGAATGATTCTCGAGAATCATTCGACTTTGGGCTGC-3′; #2: F, 5′-CCGGCGGATCTGAAATCCTTGCTTACTCGAGTAAGCAAGGATTTCAGATCCGTTTTTG-3′ and R, 5′-AATTCAAAAACGGATCTGAAATCCTTGCTTACTCGAGTAAGCAAGGATTTCAGATCCG-3′) sequences were obtained in accordance with the shRNA sequence prediction website portals. The shRNA sequences were inserted into pLKO.1-RFP vector to obtain PLKO.1-sh*FNDC3B* #1/2 plasmids. The pEnter-kana-*FNDC3B*-FLAG/His, pEnter-kana-*MYH9*-FLAG/His, and pEnter vector plasmids were obtained from Vigene Bioscience. The *FNDC3B* isoforms with short or long 3′-UTR were synthesized and cloned into pSin-EF2-puro to get pSin-EF2-puro-*FNDC3B*-long 3′-UTR or pSin-EF2-puro-*FNDC3B*-short 3′-UTR plasmids.

For transient transfection, the indicated plasmids were transfected into NPC cells using Lipofectamine 3000 reagent (Invitrogen), and then the cells were harvested for assays after at least 24 hours. For the generation of stably transfected cell lines, the PLKO.1-sh*FNDC3B* #1/2 and the vector pLKO.1-RFP, as well as the lentivirus packaging plasmids psPAX2 and pMD2.G, were cotransfected into 293FT cells using the calcium phosphate method. Lentivirus particles were harvested from the supernatant of transfected 293FT cells after 48 hours and infected SUNE-1 and HNE-1 cells. The stably transfected NPC cells were then selected using 0.5 μg/mL puromycin. The transfection efficiency was detected by western blotting assays.

2.3 | Luciferase reporter assay

The amplified *FNDC3B* short or long 3′-UTR sequences were inserted downstream of the luciferase gene in psiCHECK vector (Promega) to construct luciferase reporter plasmids. According to the manufacturer's recommendation, the luciferase reporter plasmids of *FNDC3B* with short or long 3′-UTR, plus each of 10 selective miRNA (let-7a-5p, miR-17-5p, miR-19a-3p, miR-20a-5p, miR-34c-5p, miR-93-5p, miR-106b-5p, miR-125a-5p, miR-449a, or miR-1224-5p) or miRNA control mimics (RiboBio) were cotransfected into SUNE-1 and HNE-1 cells using Lipofectamine 3000 (Invitrogen). After 24 hours, luciferase activities were detected with the Dual Luciferase Reporter Assay System (Promega), and the firefly luciferase signal was normalized to the *Renilla* signal.

For *Wnt* reporter activity assay, the pGMTCF/LEF1-Lu and pGMR-TK plasmids (Genomeditech) were cotransfected into SUNE-1 and HNE-1 cells, together with sh*FNDC3B* plasmid or its vector, or *FNDC3B* overexpressing plasmid with short or long 3′-UTR or its vector, as well as sh*FNDC3B* plasmid with MYH9 expressing plasmid or its vector. After 24 hours, recombinant murine Wnt-3a (PeproTech) was added into the medium and incubated for 24 hours. Then the luciferase activities were detected, and the firefly luciferase signal was normalized to the pGMR-TK signal.

2.4 | RNA isolation and quantitative RT-PCR

Nasopharyngeal carcinoma cell lines and tissue samples were exposed to TRIzol Reagent (Invitrogen) to extract total RNA following the manufacturer's instructions. Random primers and M-MLV reverse transcriptase (Promega) were used to synthesize the first-strand cDNA. Platinum SYBR Green qPCR SuperMix-UDG reagents (Invitrogen) were then used to amplify cDNA by the CFX96 Touch sequence detection system (Bio-Rad). The *FNDC3B* primers (F, 5′-TTGGTACCAGTGGTTATAGCCA-3′ and R, 5′-CCTTCTGGCTTACTCCACTG-3′) and *MYH9* primers (F, 5′-ATCCTGGAGGACCAGAACTGCA-3′- and R, 5′-GGCGAGGCTCTTAGATTTCTCC-3′) were used for the detection of *FNDC3B* and *MYH9* mRNA level with *GAPDH* as an endogenous control. Another 2 *FNDC3B* primers sets that were specifically designed for the "proximal site" and "distal site" were obtained from our previous study,[16] and the relative expression ratio of the "proximal site" to the "distal site" was calculated.

2.5 | Cell viability and colony formation assays

For the cell viability assay, cells (1×10^3) were counted and seeded into 96-well plates and incubated in the incubator for 0-4 days. On the indicated days, the cells were stained with 10 μL CCK-8 (Dojindo) per well, incubated in the incubator at 37°C for 2 hours and the spectrophotometer detected the absorbance of 450 nm wavelength per well. For the colony formation assay, cells (0.4×10^3) were inoculated into 6-well plates and cultured for approximately 2 weeks. Colonies were washed twice with PBS, fixed in methanol and stained with crystal violet. Colonies containing more than 50 cells were counted.

2.6 | Transwell migration and invasion assays

For the migration and invasion assays, Transwell chambers (Corning) with 8-μm pores in the membrane, coated without or with Matrigel (BD Biosciences), were separately used to explore the cell migration and invasion abilities. The harvested cells (0.5 or 1×10^5) were resuspended in serum-free medium and plated into the upper chambers for migration or invasion assays, while the lower chambers contained medium supplemented with 10% FBS. After 18-26 hours of incubation, the migrated or invaded cells were fixed with methanol, stained with crystal violet, and counted under an inverted microscope.

2.7 | Mass spectrometry and coimmunoprecipitation

Cells were lysed using the Pierce IP Lysis Buffer (Thermo Fisher Scientific) with protease inhibitor cocktail (Roche), crushed by ultrasonic cell crusher, and then centrifuged to remove the precipitation. Antibodies (2 μg) of aiti-FNDC3B (Proteintech) or anti-IgG were used to immunoprecipitate proteins overnight at 4°C. Pierce Protein A/G Magnetic Beads (Thermo Fisher Scientific) were used to recover the immune complexes. Then the immune complexes were washed by immunoprecipitation wash buffer, denatured, separated on SDS polyacrylamide gels, and stained with Coomassie blue. Huijun Biotechnology (China) undertook the mass spectrometry analysis using the target bands. Cell lysate was also immunoprecipitated with anti-IgG or anti-FLAG Abs for exogenous interaction. The expression levels of target proteins were detected by western blot analysis.

2.8 | Western blot analysis and immunofluorescent staining

For western blotting, equal amounts of proteins were separated and transferred to PVDF membranes (Millipore), and the bands were incubated with the following primary Abs: anti-FNDC3B (1:1000, 22605-1-AP; Proteintech), anti-MYH9 (1:1000, 11128-1-AP; Proteintech), anti-β-catenin (1:3000, 8480S; Cell Signaling Technology); anti-phosphorylated glycogen synthase kinase 3- (p-GSK3-β) (1:1000, Ser9, 9323S; Cell Signaling Technology), anti-GSK3-β (1:500, 9832S; Cell Signaling Technology), anti-α-tubulin Ab (1:5000, 66031-1-AP; Proteintech), anti-GAPDH Ab (1:5000, G8795; Sigma-Aldrich) overnight at 4°C, and then incubated with species-matched secondary Abs at room temperature for 1 hour for detection using chemiluminescence.

For immunofluorescent staining, cells were seeded in 24-well plates covered with sterile coverslips (Roche) for 24 hours, and incubated with anti-MYH9 Ab (1:150; Millipore) and anti-FNDC3B Ab (1:100, sc-393997; Santa Cruz Biotechnology). Then cells were incubated with Alexa Fluor 594 IgG secondary Ab (1:1000, A21207; Life Technologies) and Alexa Fluor 488 IgG secondary Ab (1:1000, A21202; Life Technologies). The nuclei were then counterstained with DAPI, and images were captured using a confocal laser scanning microscope (Olympus FV1000).

2.9 | Animal models, immunohistochemistry, and H&E staining

BALB/c-nu mice aged 4-6 weeks were purchased from Charles River Laboratories. For xenograft tumor growth model, the right dorsal flank of the mice was s.c. inoculated with SUNE-1 cells (1×10^6) stably knocking down *FNDC3B* or not, as well as overexpressing *FNDC3B* with long or short 3′-UTR or vector. Subcutaneous tumor size was measured every 3 days to calculate the tumor volumes. The mice were killed after 4 weeks, and the tumors were excised, weighed,

and paraffin-embedded. Then the sections were stained with anti-MYH9 (1:800; Proteintech), anti-FNDC3B (1:100; Proteintech), or anti-β-catenin (1:200; Proteintech) Ab for immunohistochemistry assay.

For the lung metastatic colonization model, SUNE-1 cells (1×10^6) that stably knocking down *FNDC3B* or not were i.v. inoculated through the tail vein of mice. The mice were killed after 8 weeks, and the lung tissues were excised to observe and count the number of macroscopic metastatic nodes formed on the lungs. Then, lung tissues were paraffin-embedded for H&E staining and immunohistochemistry analysis. All of the animal experiments were carried out according to the guidelines of the Experimental Animal Care and Use Committee of Sun Yat-sen University Cancer Center.

2.10 | Statistical analyses

Our statistical analyses were all undertaken using SPSS 22.0 software (IBM) or GraphPad Prism 6 (version 8.0). The data representing results of at least 3 independent experiments were expressed as the mean ± SD. Two-tailed unpaired Student's *t* test was used to analyze differences between 2 groups, and $P < .05$ was considered significant.

3 | RESULTS

3.1 | *FNDC3B* isoform with shorter 3′-UTR escapes from miRNA-mediated gene repression

Based on our previous APA sites sequencing data, we found that *FND3CB* tended to use the proximal polyadenylation site and produce shorter 3′-UTR.[16] As a transcript with shorter 3′-UTR can result in the loss of miRNA-targeting sites and escape from miRNA-mediated gene repression, we analyzed putative miRNA-targeting sites on the *FNDC3B* 3′-UTR using PITA, Pictar, and TargetScan algorithms on the starBase version 2.0 website. We then analyzed our previous microarray data[17] and selected differentially expressed miRNAs (fold change greater than 1.5, $P < .05$) between 312 NPC and 18 normal nasopharynx tissues. Combining the above 2 analyses, we screened 24 miRNAs which is dysregulated in NPC tissues and can bind to *FNDC3B* 3′-UTR (Figure 1A). As shown in Figure 1B, most of the miRNA-targeting sites were presented on the longer 3′-UTR but not the shorter 3′-UTR. We subsequently selected 10 miRNAs for luciferase reporter assays. The luciferase activity of *FNDC3B* isoform with longer 3′-UTR was obviously reduced by overexpression of each of the selected miRNAs compared to the negative control (Figure 1C). However, this suppressive effect was not observed in the reporter plasmid of *FNDC3B* shorter 3′-UTR isoform (Figure 1D). These results indicate that APA-induced *FND3CB* 3′-UTR shortening could escape from miRNA-mediated gene repression.

We then tested *FNDC3B* expression in 7 NPC cell lines and the normal immortalized nasopharynx epithelial cell NP69 using quantitative RT-PCR and western blot analysis, and found that *FNDC3B* was significantly increased at both the mRNA and protein levels (Figure 1E). Then we validated that *FNDC3B* was more likely to use proximal polyadenylation site and produce shorter 3′-UTR in NPC cell lines than NP69, and FNDC3B protein abundance was negatively correlated with its 3′-UTR length (Figure 1F). We further detected the mRNA and protein levels of *FNDC3B* in 8 normal nasopharyngeal epithelial tissue and 12 NPC tissue samples, and found that both the mRNA and protein levels of *FNDC3B* in NPC tissues were higher (Figure 1G). These results suggest that *FNDC3B* is upregulated and might function as an oncogene in NPC.

3.2 | Knockdown of *FNDC3B* suppresses NPC cell proliferation, migration, and invasion

To illustrate the effect of knocking down *FNDC3B* on NPC cell proliferative, migratory, and invasive abilities, 2 sh*FNDC3B* plasmids were constructed and transiently transfected into SUNE-1 and HNE-1 cells to undertake CCK-8, colony formation, Transwell migration, and invasion assays. Figure 2A shows the knockdown efficiencies of 2 sh*FNDC3B* plasmids in SUNE-1 and HNE-1 cells. The CCK-8 assay showed that knockdown of *FNDC3B* significantly decreased the growth rate of both SUNE-1 and HNE-1 cells (Figure 2B). The colony formation assay showed that inhibition of *FNDC3B* remarkably decreased the number of colonies (Figure 2C). As determined by the Transwell migration and invasion assays, both SUNE-1 and HNE-1 cells transiently transfected with sh*FNDC3B* migrated and invaded more slowly compared to the control group (Figure 2D,E). These findings suggest that the proliferative, migratory, and invasive abilities of NPC cells would be inhibited after knocking down *FNDC3B*.

FIGURE 1 *FNDC3B* with shorter 3′-UTR escapes from microRNA (miRNA)-mediated gene repression. A, Screened miRNAs that were differentially expressed in nasopharyngeal carcinoma (NPC) and could bind to the *FNDC3B* 3′-UTR based on microarray data analysis and the starBase version 2.0 website. B, Binding sites of screened miRNAs on the 3′-UTR region of *FNDC3B*. CDS, coding DNA sequence. C, D, Relative luciferase activities of SUNE-1 and HNE-1 cells transfected with luciferase reporter plasmids of *FNDC3B* with shorter (C) or longer 3′-UTR (D) plus each of the selected miRNA mimics or negative control. E, Quantitative RT-PCR and western blot analysis of *FNDC3B* expression in NPC cell lines and the normal NP69 cell line. F, Quantification analysis of *FNDC3B* 3′-UTR length and its correlation with FNDC3B protein abundance in NPC cell lines and the normal NP69 cell line. G, Quantitative RT-PCR and western blot analysis of *FNDC3B* expression in NPC (n = 12) and normal nasopharynx tissues (n = 8). All of the data are presented as the mean ± SD; Student's *t* test was used to calculate *P* values. *$P < .05$

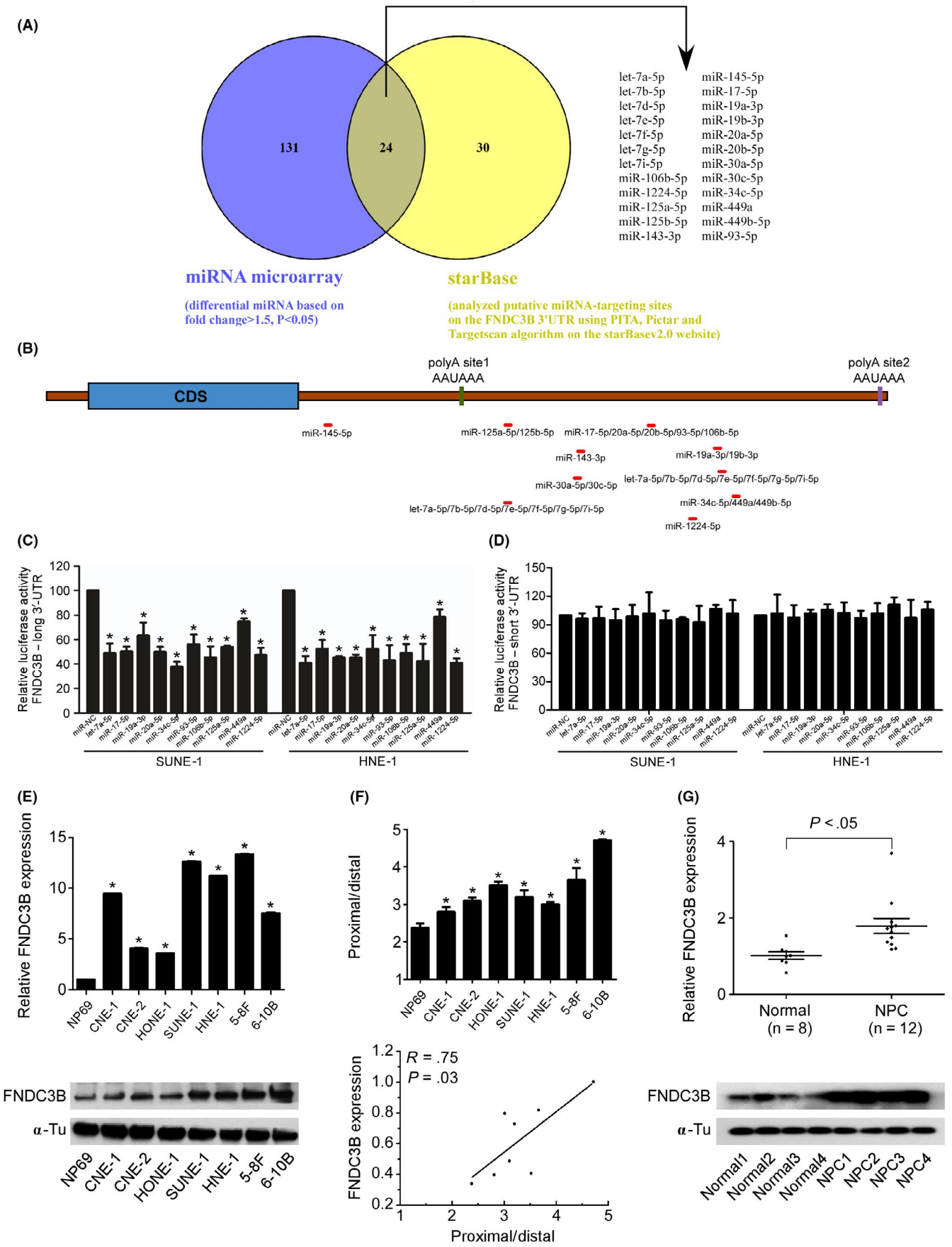
(A)
131
24
30
let-7a-5p
let-7b-5p
let-7d-5p
let-7e-5p
let-7f-5p
let-7g-5p
let-7i-5p
miR-106b-5p
miR-1224-5p
miR-125a-5p
miR-125b-5p
miR-143-3p
miR-145-5p
miR-17-5p
miR-19a-3p
miR-19b-3p
miR-20a-5p
miR-20b-5p
miR-30a-5p
miR-30c-5p
miR-34c-5p
miR-449a
miR-449b-5p
miR-93-5p
miRNA microarray
(differential miRNA based on fold change>1.5, P<0.05)
starBase
(analyzed putative miRNA-targeting sites on the FNDC3B 3'UTR using PITA, Pictar and Targetscan algorithm on the starBasev2.0 website)
(B)
CDS
polyA site1 AAUAAA
polyA site2 AAUAAA
miR-145-5p
miR-125a-5p/125b-5p
miR-17-5p/20a-5p/20b-5p/93-5p/106b-5p
miR-143-3p
miR-19a-3p/19b-3p
miR-30a-5p/30c-5p
let-7a-5p/7b-5p/7d-5p/7e-5p/7f-5p/7g-5p/7i-5p
miR-34c-5p/449a/449b-5p
let-7a-5p/7b-5p/7d-5p/7e-5p/7f-5p/7g-5p/7i-5p
miR-1224-5p
(C)
Relative luciferase activity FNDC3B – long 3'-UTR
miR-NC
let-7a-5p
miR-17-5p
miR-19a-3p
miR-20a-5p
miR-34c-5p
miR-93-5p
miR-106b-5p
miR-125a-5p
miR-449a
miR-1224-5p
SUNE-1
HNE-1
(D)
Relative luciferase activity FNDC3B – short 3'-UTR
(E)
Relative FNDC3B expression
NP69
CNE-1
CNE-2
HONE-1
SUNE-1
HNE-1
5-8F
6-10B
FNDC3B
α-Tu
(F)
Proximal/distal
R = .75
P = .03
FNDC3B expression
(G)
P < .05
Relative FNDC3B expression
Normal (n = 8)
NPC (n = 12)
Normal1
Normal2
Normal3
Normal4
NPC1
NPC2
NPC3
NPC4

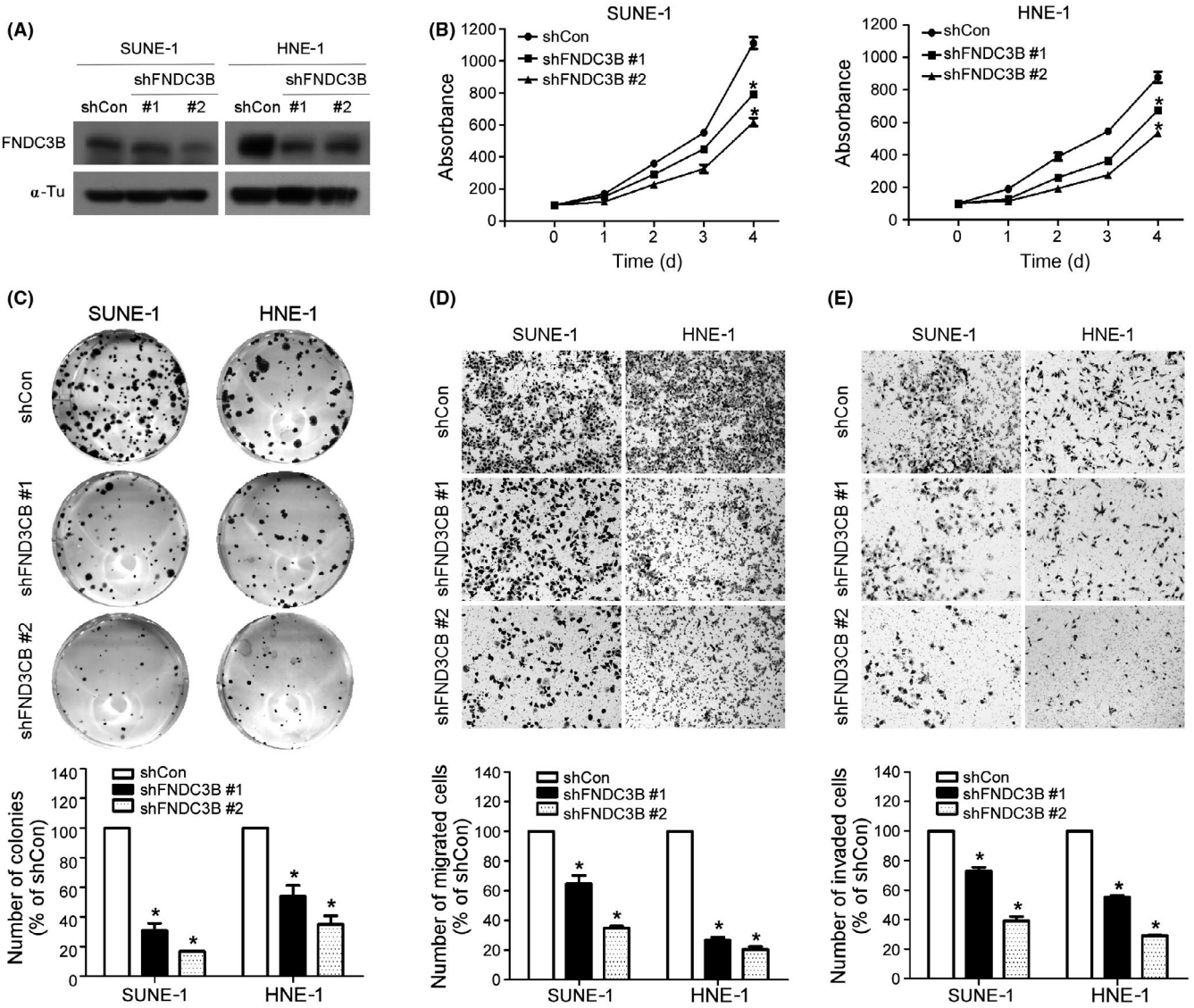

FIGURE 2 Knockdown of *FNDC3B* suppresses nasopharyngeal carcinoma proliferation, migration, and invasion. A, FNDC3B expression determined by western blot analysis after transfection with sh*FNDC3B*s or vector. B, Results of CCK-8 assay in SUNE-1 and HNE-1 cells transiently knocking down *FNDC3B* or not (shCon). C, Representative images and quantification of colony formation assay in SUNE-1 and HNE-1 cells transiently knocking down *FNDC3B* or not. D, E, Representative images and quantification of Transwell migration (D) and invasion (E) assays in SUNE-1 and HNE-1 cells transiently knocking down *FNDC3B* or not. Data are presented as the mean ± SD; Student's *t* test was used to calculate *P* values. $^*P < .05$

3.3 | *FNDC3B*, especially its isoform with shorter 3′-UTR, promotes NPC progression

To determine whether ectopic expression of *FNDC3B* affects the proliferative, migratory, and invasive abilities of NPC cells, we first established SUNE-1 and HNE-1 cells stably knocking down *FNDC3B* with sh*FNDC3B* #2 plasmid, and then transiently transfected with the *FNDC3B* or vector plasmids (Figure 3A). The CCK-8 and colony formation assays showed that overexpression of *FNDC3B* prominently increased the NPC cell proliferation and colony formation rates (Figure 3B,C). Meanwhile, ectopic expression of *FNDC3B* in both SUNE-1 and HNE-1 cells markedly increased the number of migratory and invasive cells as determined by the Transwell migration and invasion assays (Figure 3D,E).

Furthermore, we transiently transfected *FNDC3B* plasmid with longer 3′-UTR, *FNDC3B* plasmid with shorter 3′-UTR or its vector plasmid into SUNE-1 and HNE-1 cells with stable *FNDC3B* knockdown to undertake the functional experiments (Figure 3F). Our functional assays showed that both *FNDC3B* transcripts with longer and shorter 3′-UTR could promote NPC proliferation, migration, and invasion, and the effect of *FNDC3B* transcripts with shorter 3′-UTR was greater (Figure 3G-J). These results indicate that overexpression of *FNDC3B*, especially its shorter 3′-UTR transcript, can promote NPC progression.

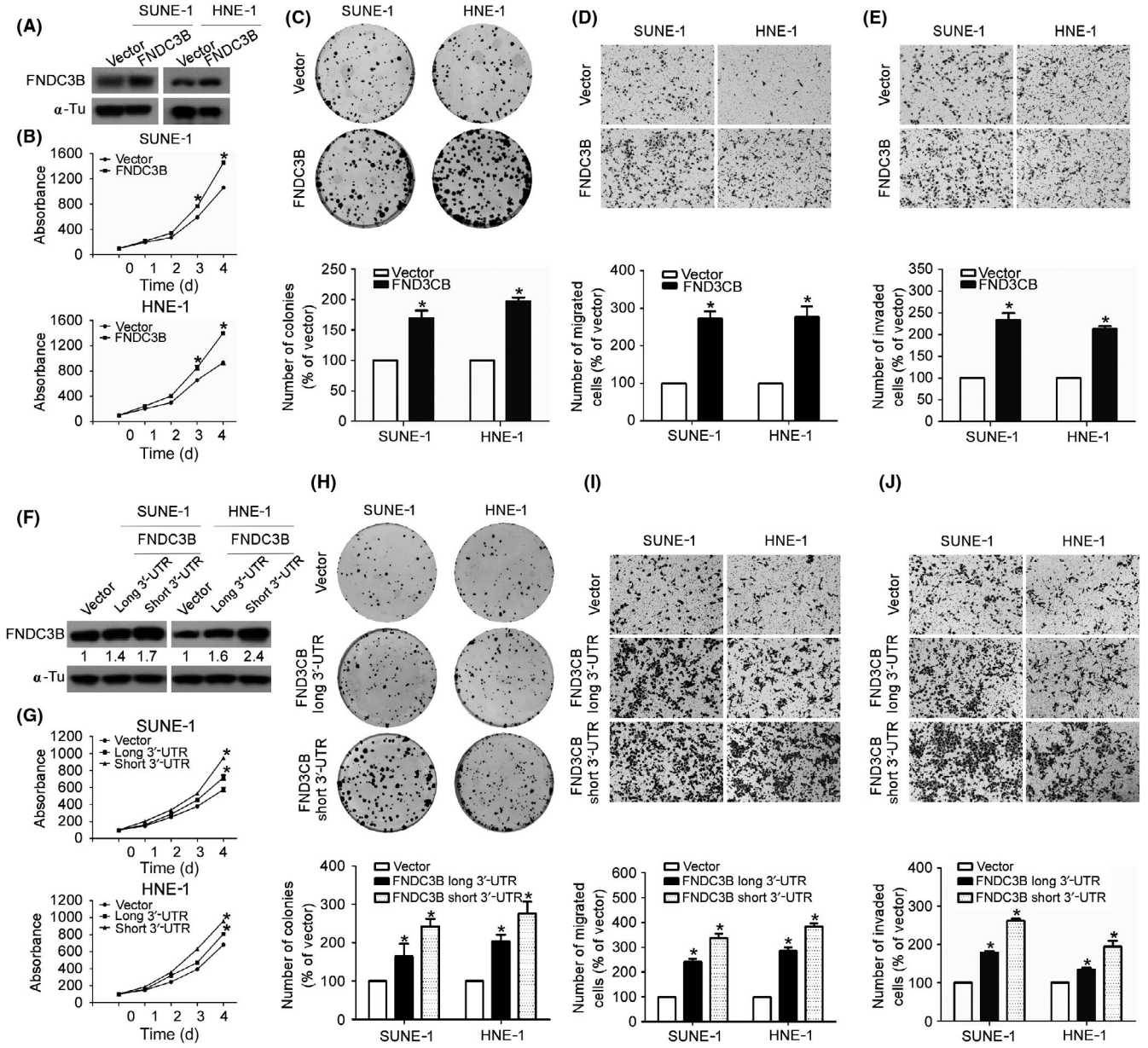

FIGURE 3 *FNDC3B*, especially its isoform with short 3′-UTR, promotes nasopharyngeal carcinoma progression. A, FNDC3B expression determined by western blot analysis after transfection with *FNDC3B* or vector. B-E, CCK-8 (B), colony formation (C), Transwell migration (D), and invasion (E) assays in SUNE-1 and HNE-1 cells overexpressing *FNDC3B* or not (shCon). F, FNDC3B expression determined by western blot analysis after transfection with *FNDC3B* long 3′-UTR, *FNDC3B* short 3′-UTR, or vector. G-J, CCK-8 (G), colony formation (H), Transwell migration (I), and invasion (J) assays undertaken in SUNE-1 and HNE-1 cells expressing *FNDC3B* long 3′-UTR, *FNDC3B* short 3′-UTR, or vector. Data are presented as the mean ± SD; Student's *t* test was used to calculate *P* values. *$P < .05$

3.4 | FNDC3B upregulates MYH9 and stimulates the Wnt/β-catenin signaling pathway

To further explore the mechanism of *FNDC3B* affecting on NPC proliferative, migratory, and invasive abilities, we undertook coimmunoprecipitation of anti-FNDC3B in SUNE-1 cells, and then carried out liquid chromatography-tandem mass spectrometry using the differential gel bands (Figure 4A). Among the proteins associated with FNDC3B, MYH9 had the highest interaction score and was selected for further analysis (data not shown). *MYH9* has been reported to function as an oncogene in most types of cancer, and it plays an important role in tumor cell adhesion, migration, and proliferation.[18-20] The exogenous and endogenous coimmunoprecipitation showed that FNDC3B could physically interact with MYH9 (Figure 4B), which was verified by the immunofluorescence staining that FNDC3B was colocalized with MYH9 in the cytoplasm of both SUNE-1 and HNE-1 cells (Figure 4C).

Furthermore, western blot analysis validated that MYH9 protein was upregulated in NPC cell lines and tissue samples (Figure 4D). Quantitative RT-PCR showed that neither knocking down nor overexpression of *FNDC3B* could affect the *MYH9* mRNA levels (Figure 4E). However, knockdown of *FNDC3B* inhibited the expression of

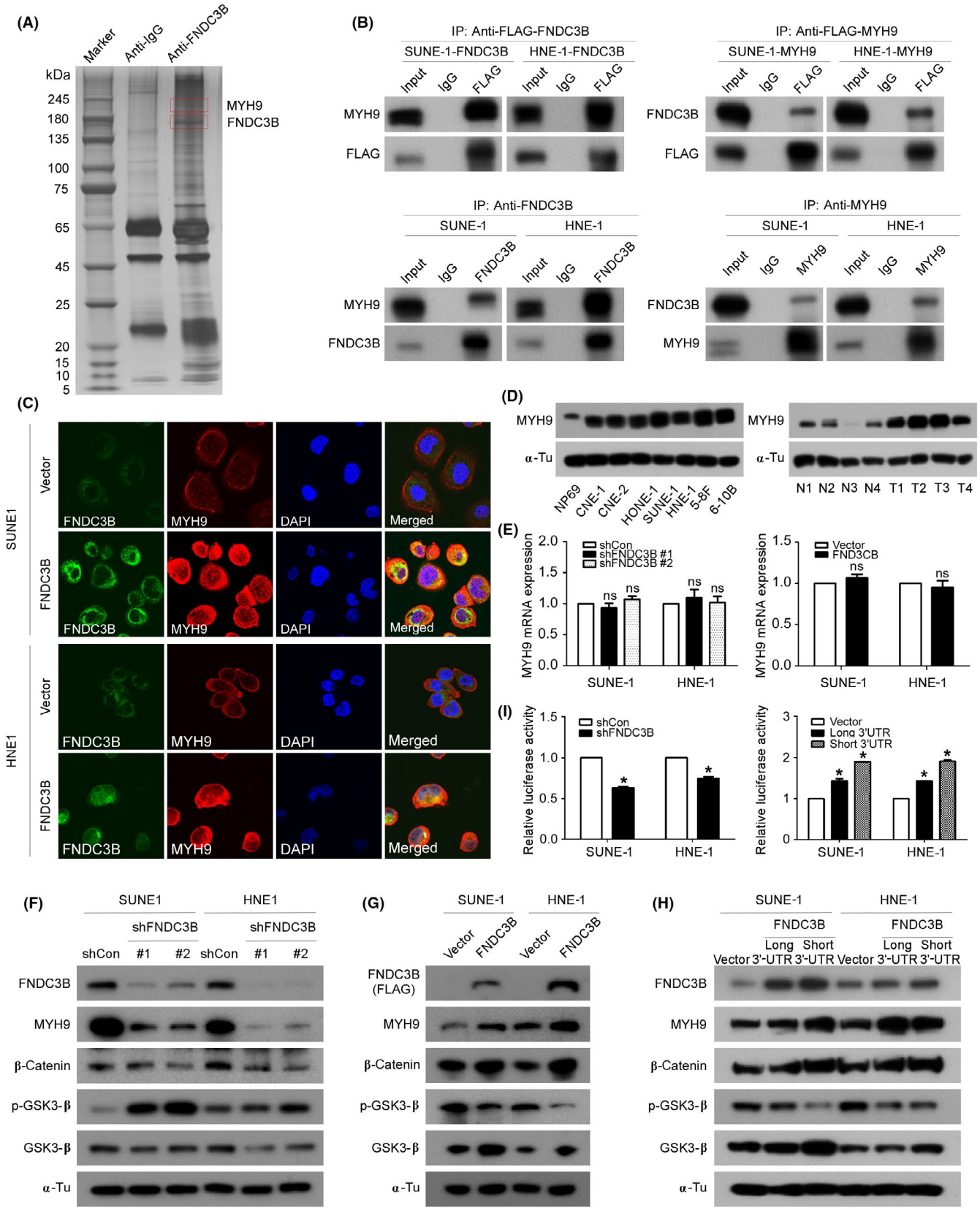

MYH9, β-catenin, and total GSK-3β, but increased the expression of p-GSK-3β; and ectopic expression of *FND3CB* had opposite effects (Figure 4F,G). In addition, both *FNDC3B* transcripts with longer and shorter 3′-UTR increased MYH9, β-catenin, and GSK-3β levels, but decreased p-GSK-3β level, and the effect of *FNDC3B* transcript with shorter 3′-UTR, was greater (Figure 4H). Finally, knockdown of

FIGURE 4 *FNDC3B* upregulates *MYH9* and stimulates Wnt/β-catenin signaling pathway. A, FNDC3B-immunoprecipitated proteins of SUNE-1 cells were separated by SDS-PAGE; red boxes indicate proteins of interest. B, Exogenous and endogenous interactions between FNDC3B and MYH9 verified by coimmunoprecipitation (IP) with anti-FLAG or anti-FNDC3B and anti-MYH9 Abs in SUNE-1 and HNE-1 cells. C, Cellular colocalization of MYH9 (red) and FNDC3B (green) determined by immunofluorescence staining. D, Expression of MYH9 detected by western blot analysis in nasopharyngeal carcinoma cell lines and tissue samples. E, Quantitative RT-PCR analysis of the mRNA expression of *MYH9* in SUNE-1 and HNE-1 cells after knocking down *FNDC3B* or not, as well as overexpressing *FNDC3B* or not. F-H, Western blot analysis of the expression levels of FNDC3B, MYH9, β-catenin, phosphorylated glycogen synthase kinase 3 (p-GSK-3β), and total GSK-3β in SUNE-1 and HNE-1 cells knocking down *FNDC3B* or not (F), overexpressing *FNDC3B* or not (G), as well as expressing *FNDC3B* long 3′-UTR, *FNDC3B* short 3′-UTR, or vector (H). I, Relative luciferase activities of Wnt reporter plasmid in SUNE-1 and HNE-1 cells after knocking down *FNDC3B* or not, as well as overexpressing of *FNDC3B* or not. Data are presented as the mean ± SD; Student's *t* test was used to calculate *P* values. *$P < .05$. ns, not significant

FNDC3B inhibited the luciferase activity of Wnt reporter plasmids, whereas overexpression of FNDC3B, especially those with short 3′-UTR, enhanced the luciferase activity of Wnt reporter plasmids (Figure 4I). These results indicate that *FNDC3B* can bind to and stabilize MYH9 to stimulate the Wnt/β-catenin signaling pathway.

3.5 | MYH9 reverses the inhibitory effect of *FNDC3B* knockdown on NPC progression

To test whether MYH9 mediates the tumor suppressive effect of *FNDC3B* knockdown in NPC, we established SUNE-1 and HNE-1 cells stably knocking down *FNDC3B*, and then transiently transfected them with the *MYH9* or vector plasmids to undertake a series of functional experiments. The results showed that overexpression of *MYH9* reversed the inhibitory effect of *FNDC3B* knockdown on NPC cell proliferation, migration, and invasion (Figure 5A-H). In addition, ectopic expression of *MYH9* reversed the inactivation effect of *FNDC3B* knockdown on the Wnt/β-catenin pathway (Figure 5I-K). These results suggest that *FNDC3B* can promote NPC progression by upregulating MYH9 to stimulate the Wnt/β-catenin pathway.

3.6 | *FNDC3B* promotes NPC tumor growth and lung metastasis in vivo

To elucidate the effect of knockdown of *FNDC3B* on NPC tumor growth and metastasis in vivo, we used SUNE-1 cells stably transfected with sh*FNDC3B* #2 or the shCon (control) plasmid to construct xenograft tumor growth and lung metastasis colonization models. As shown in Figure 6A,B the mice in the sh*FNDC3B* group formed tumors with smaller volumes and lower weights than the control group. Additionally, the immunohistochemical sections showed that the formed tumors in the sh*FNDC3B* group expressed lower FNDC3B, MYH9, and β-catenin than the control group, suggesting that FNDC3B can increase MYH9 expression and activate the Wnt/β-catenin signaling in vivo (Figure 6C). The lung metastasis colonization assay showed that the tumor nodules formed on the lungs of the sh*FNDC3B* mice were notably fewer and smaller than the control mice (Figure 6D), which was validated by H&E staining (Figure 6E). Simultaneously, both FNDC3B and MYH9 were synergistically expressed lower in the metastatic lung nodules of the sh*FNDC3B* group (Figure 6F). In addition, both FNDC3B transcripts with longer and shorter 3′-UTR could promote xenograft tumor growth, and the effect of FNDC3B transcript with shorter 3′-UTR was greater (Figure 6G,H). These data indicate that *FNDC3B* can promote NPC tumor growth and lung metastasis by downregulating *MYH9* and stimulate the Wnt/β-catenin pathway in vivo.

4 | DISCUSSION

Almost all mRNAs, except for histone mRNAs, in eukaryotic cells have a polyadenylation (polyA) tail. Alternative polyadenylation is a phenomenon that a gene might have multiple different polyA loci, and more than half of the genes have APA sites in the human genome.[21] Alternative polyadenylation plays an important role in tumorigenesis, and the 3′-UTR shortening is prevalent in multiple kinds of tumors.[6,7] As we known, 3′-UTRs contain multiple cis-elements, such as U-rich or Au-rich elements, polyA signal, and miRNA target sites.[22] The APA-induced changes in 3′-UTR length could result in the loss or acquisition of regulatory motifs, and bring a series of changes in cellular biological function.[23] Recently, it has been reported that loss of NUDT21 increased usage of proximal polyadenylation sites and produced shorter 3′-UTR in various oncogenes, such as *PSMB2* and *CXXC5*, which had fewer miRNA binding sites, escaped from miRNA-mediated gene repression, and further promoted hepatocellular cancer cell proliferation and invasion.[11,12] In addition, the 3′-UTR shortening of *RAC1* induced by *CSTF2* promoted bladder cancer cell proliferation, migration, and invasion.[13] Our previous sequencing study showed that *FND3CB* tended to use the proximal polyadenylation site and produce shorter 3′-UTR in NPC. In our present study, we screened 24 miRNAs that can bind to *FNDC3B* 3′-UTR and most of the miRNA targeting sites were presented on the longer 3′-UTR but not the shorter 3′-UTR. Luciferase reporter assay indicated that *FNDC3B* isoform with shorter 3′-UTR could escape from miRNA-mediated gene repression, which contributed to the upregulation of *FNDC3B* in NPC.

FNDC3B, also known as FAD104 (factor for adipocyte differentiation 104), is located at 3q26, and is amplified in more than 20% of human tumors.[24,25] Recently, *FNDC3B* was found to serve as an oncogene and it can promote tumorigenesis and metastasis in various cancer types.[24-28]*FNDC3B* can promote cell migration and metastasis by cooperating with annexin A2 (ANXA2) in hepatocellular carcinoma.[26]*FNDC3B* is correlated with poor survival and can promote epithelial-mesenchymal transition in lung adenocarcinoma.[27]*FNDC3B*

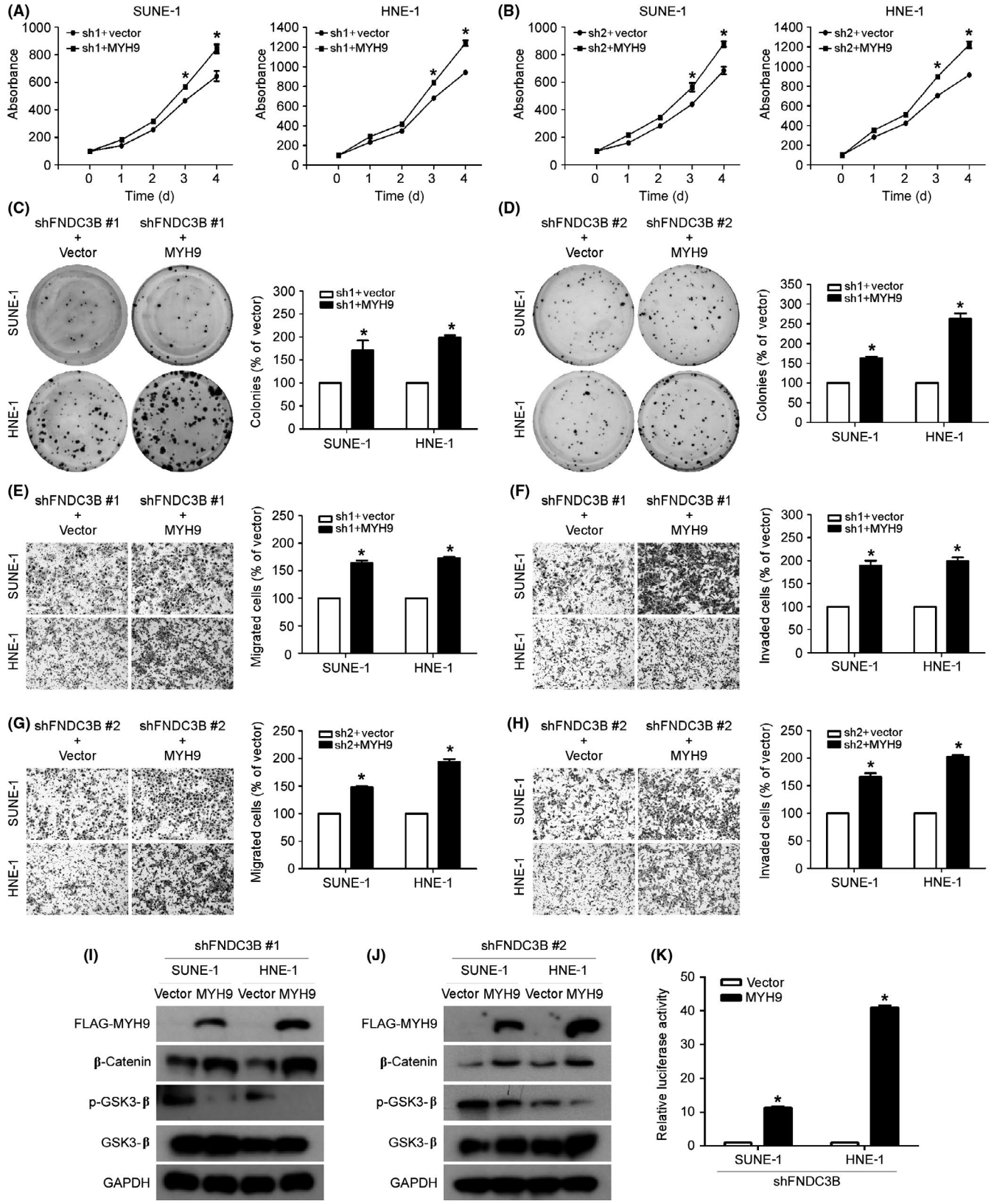

FIGURE 5 *MYH9* reverses the inhibitory effect of *FNDC3B* knockdown on nasopharyngeal carcinoma progression. A-H, CCK-8 (A, B), colony formation (C, D), Transwell migration (E, F), and invasion (G, H) assays undertaken in *FNDC3B* stably knocking down SUNE-1 and HNE-1 cells transfected with MYH9 or vector. All data are presented as the mean ± SD; Student's *t* test was used to calculate *P* values. I, J, Western blot analysis of the levels of FNDC3B, MYH9, β-catenin, phosphorylated glycogen synthase kinase 3 (p-GSK-3β), and total GSK-3β in *FNDC3B* stably knocking down SUNE-1 and HNE-1 cells transfected with MYH9 or vector. K, Relative luciferase activities of Wnt reporter plasmid in *FNDC3B* stably knocking down SUNE-1 and HNE-1 cells transfected with MYH9 or vector. All data are presented as the mean ± SD; Student's *t* test was used to calculate *P* values. *$P < .05$

can promote migration and invasion in tongue squamous cell carcinoma.[28] In addition, Fan et al found that there was a binding site for miR-143 in the 3′-UTR region of *FNDC3B*, which was involved in the regulation of prostate cancer metastasis.[29] Furthermore, Hong et al found that *FNDC3B* circular RNA could promote the migration and invasion of gastric cancer cells by reducing E-cadherin

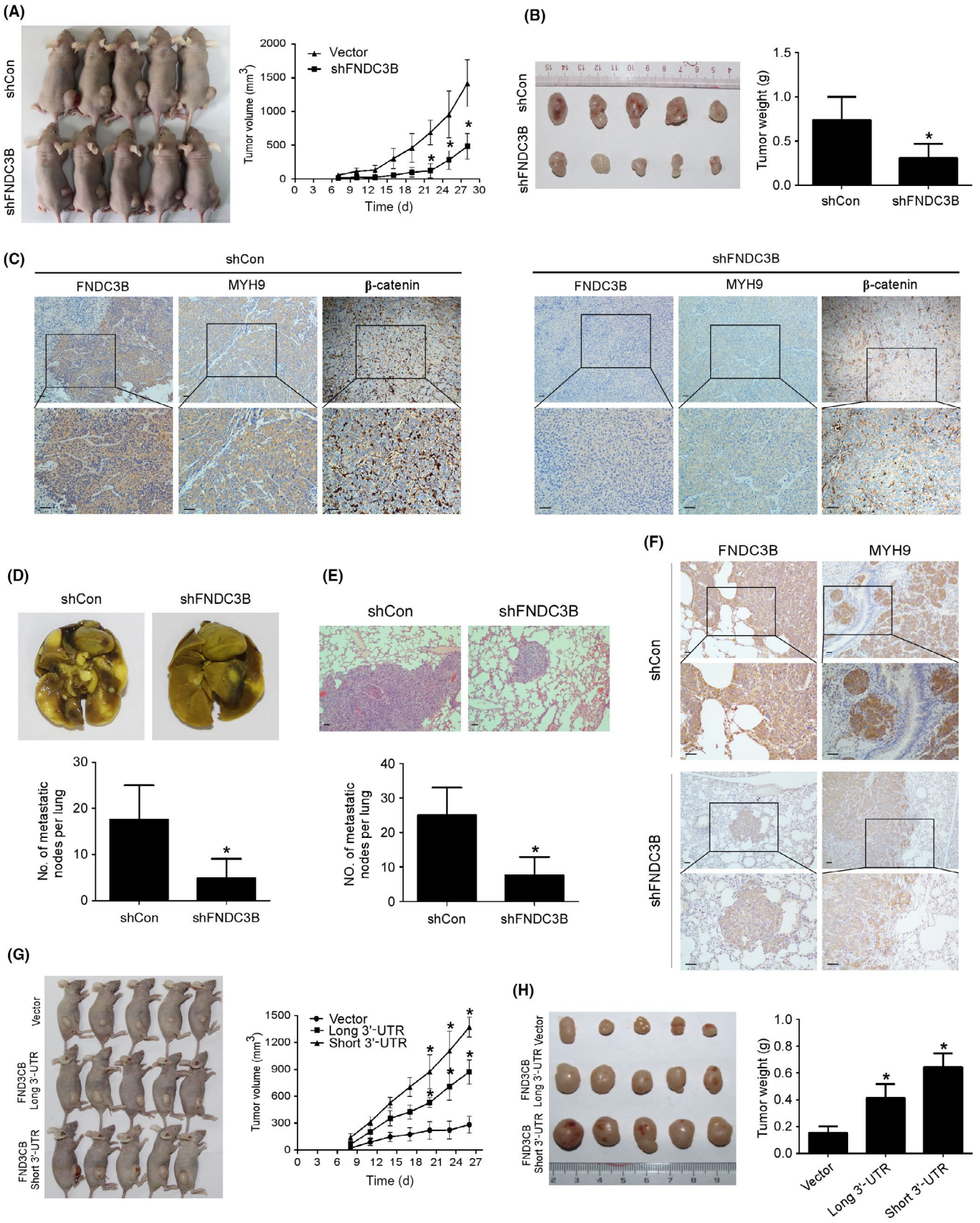

FIGURE 6 *FNDC3B* promotes nasopharyngeal carcinoma tumor growth and lung metastasis in vivo. A-C, Right dorsal flank of mice was s.c. inoculated with SUNE-1 cells stably transfected with sh*FNDC3B*#2 or the vector plasmid to construct the xenograft tumor growth models. A-C, Representative images of formed tumors and growth curves of tumor volumes (A), excised tumors and their weights (B), as well as expression of FNDC3B, MYH9, and β-catenin in xenograft tumors (C). D, E, SUNE-1 cells stably transfected with sh*FNDC3B*#2 or the vector plasmid were i.v. inoculated through the tail vein of mice to establish lung metastatic colonization models. Representative images and quantification of macroscopic tumor nodules formed on the lung surface (D), and microscopic tumor nodules in the lung tissue stained with H&E (E). F, G, Right dorsal flank of mice s.c. inoculated with SUNE-1 cells stably transfected with *FNDC3B* long 3′-UTR, *FNDC3B* short 3′-UTR, or the vector plasmid to construct the xenograft tumor growth models. Representative images of the formed tumors and its growth curves of tumor volumes (F), the excised tumors and their weights (G). Scale bar, 50 μm. Data are presented as the mean ± SD; Student's *t* test was used to calculate *P* values. $^*P < .05$

expression and enhancing CD44 expression.[30] In the present study, we investigated the biological function of *FNDC3B* in NPC. The findings showed that knocking down *FNDC3B* inhibited NPC cell proliferation, migration, and invasion, whereas overexpression of *FNDC3B* exerted the opposite effects. In addition, we found that *FNDC3B* with shorter 3′-UTR could promote more aggressive malignant behaviors than those with longer 3′-UTR. Herein, our investigations enriched the role of *FNDC3B* in human cancers.

The tumor metastasis-associated protein MYH9 is an isoform of the non-muscle II (NM II) family of proteins.[31] As a skeleton protein, MYH9 plays an important role in cell adhesion, polarity, migration, and proliferation through mediating the actin-based contractile motion.[32]*MYH9* is recognized as an oncogene, as it is closely related to the progress and poor prognosis of most solid tumors.[18-20] For example, *MYH9* overexpression was induced by LIM kinase 1 (LIMK1) and promoted growth and metastasis by activating MAPK/AKT signaling in colorectal cancer.[33,34] The S100A4-MYH9 axis could promote migration and invasion through inducing transforming growth factor-β-mediated epithelial-mesenchymal transition in gastric cancer.[35] In addition, MYH9 was downregulated by miR-124, miR-647, or let-7f to suppress invasion and metastasis in colorectal or gastric cancer.[36-38] It is well known that the Wnt/β-catenin signaling can promote metastasis and is associated with poor progression in a variety of cancer types, including NPC.[39,40] Our present findings revealed that MYH9 was upregulated and positively correlated with FNDC3B expression in NPC. Further study revealed that FNDC3B could increase MYH9 expression and activate the Wnt/β-catenin signaling pathway to promote NPC proliferation, migration, and invasion in NPC.

In conclusion, our research showed that APA-induced *FNDC3B* 3′-UTR shortening could escape from miRNA-mediated gene repression and contributed to its high expression in NPC. *FNDC3B*, especially its isoform with shorter 3′-UTR, promoted NPC proliferation and invasion by upregulating MYH9 expression and stimulating the Wnt/β-catenin signaling pathway. These results suggested that the newly identified *FNDC3B*-*MYH9*-Wnt/β-catenin axis could represent potential targets for individualized treatment in NPC.

ACKNOWLEDGMENTS

This work was supported by grants from the National Natural Science Foundation of China (81572962 and 81802705), Key-Area Research and Development Program of Guangdong Province (2019B020230002), Natural Science Foundation of Guangdong Province (2017A030312003 and 2017A030310468), Health and Medical Collaborative Innovation Project of Guangzhou City, China (201803040003), and SZU Medical Young Scientists Program. All of the data from this study have been deposited at Sun Yat-sen University Cancer Center with the reference number RDDB202000833.

CONFLICT OF INTEREST

The authors declare that they have no competing interests.

ORCID

Ling-Long Tang https://orcid.org/0000-0002-8561-1454
Na Liu https://orcid.org/0000-0001-8654-3636

REFERENCES

1. Bray F, Ferlay J, Soerjomataram I, Siegel RL, Torre LA, Jemal A. Global cancer statistics 2018: GLOBOCAN estimates of incidence and mortality worldwide for 36 cancers in 185 countries. *CA Cancer J Clin*. 2018;68:394-424.
2. Lee AW, Ma BB, Ng WT, Chan AT. Management of nasopharyngeal carcinoma: Current practice and future perspective. *J Clin Oncol*. 2015;33:3356-3364.
3. Chua MLK, Wee JTS, Hui EP, Chan ATC. Nasopharyngeal carcinoma. *Lancet*. 2016;387:1012-1024.
4. Proudfoot NJ. Ending the message: poly(A) signals then and now. *Genes Dev*. 2011;25:1770-1782.
5. Sandberg R, Neilson JR, Sarma A, Sharp PA, Burge CB. Proliferating cells express mRNAs with shortened 3' untranslated regions and fewer microRNA target sites. *Science*. 2008;320:1643-1647.
6. Mayr C, Bartel DP. Widespread shortening of 3'UTRs by alternative cleavage and polyadenylation activates oncogenes in cancer cells. *Cell*. 2009;138:673-684.
7. Lin Y, Li Z, Ozsolak F, et al. An in-depth map of polyadenylation sites in cancer. *Nucleic Acids Res*. 2012;40:8460-8471.
8. Xia Z, Donehower LA, Cooper TA, et al. Dynamic analyses of alternative polyadenylation from RNA-seq reveal a 3'-UTR landscape across seven tumour types. *Nat Commun*. 2014;5:5274.
9. Park HJ, Ji P, Kim S, et al. 3' UTR shortening represses tumor-suppressor genes in trans by disrupting ceRNA crosstalk. *Nat Genet*. 2018;50:783-789.
10. Kataoka K, Shiraishi Y, Takeda Y, et al. Aberrant PD-L1 expression through 3'-UTR disruption in multiple cancers. *Nature*. 2016;534:402-406.
11. Sun M, Ding J, Li D, Yang G, Cheng Z, Zhu Q. NUDT21 regulates 3'-UTR length and microRNA-mediated gene silencing in hepatocellular carcinoma. *Cancer Lett*. 2017;410:158-168.
12. Tan S, Li H, Zhang W, et al. NUDT21 negatively regulates PSMB2 and CXXC5 by alternative polyadenylation and contributes to hepatocellular carcinoma suppression. *Oncogene*. 2018;37:4887-4900.

13. Chen X, Zhang JX, Luo JH, et al. CSTF2-induced shortening of the RAC1 3'UTR promotes the pathogenesis of urothelial carcinoma of the bladder. *Cancer Res*. 2018;78:5848-5862.
14. Lembo A, Di Cunto F, Provero P. Shortening of 3'UTRs correlates with poor prognosis in breast and lung cancer. *PLoS ONE*. 2012;7:e31129.
15. Morris AR, Bos A, Diosdado B, et al. Alternative cleavage and polyadenylation during colorectal cancer development. *Clin Cancer Res*. 2012;18:5256-5266.
16. Xu YF, Li YQ, Liu N, et al. Differential genome-wide profiling of alternative polyadenylation sites in nasopharyngeal carcinoma by high-throughput sequencing. *J Biomed Sci*. 2018;25:74.
17. Liu N, Chen NY, Cui RX, et al. Prognostic value of a microRNA signature in nasopharyngeal carcinoma: a microRNA expression analysis. *Lancet Oncol*. 2012;13:633-641.
18. Katono K, Sato Y, Jiang SX, et al. Prognostic significance of MYH9 expression in resected non-small cell lung cancer. *PLoS ONE*. 2015;10: e0121460.
19. Liu L, Yi J, Deng X, et al. MYH9 overexpression correlates with clinicopathological parameters and poor prognosis of epithelial ovarian cancer. *Oncol Lett*. 2019;18:1049-1056.
20. Yu M, Wang J, Zhu Z, et al. Prognostic impact of MYH9 expression on patients with acute myeloid leukemia. *Oncotarget*. 2017;8:156-163.
21. Tian B, Hu J, Zhang H, Lutz CS. A large-scale analysis of mRNA polyadenylation of human and mouse genes. *Nucleic Acids Res*. 2005;33:201-212.
22. Sun Y, Fu Y, Li Y, Xu A. Genome-wide alternative polyadenylation in animals: insights from high-throughput technologies. *J Mol Cell Biol*. 2012;4:352-361.
23. Lutz CS. Alternative polyadenylation: a twist on mRNA 3' end formation. *ACS Chem Biol*. 2008;3:609-617.
24. Szeliga M, Obara-Michlewska M, Matyja E, et al. Transfection with liver-type glutaminase cDNA alters gene expression and reduces survival, migration and proliferation of T98G glioma cells. *Glia*. 2009;57:1014-1023.
25. Cai C, Rajaram M, Zhou X, et al. Activation of multiple cancer pathways and tumor maintenance function of the 3q amplified oncogene FND3CB. *Cell Cycle*. 2012;11:1773-1781.
26. Lin CH, Lin YW, Chen YC, et al. FNDC3B promotes cell migration and tumor metastasis in hepatocellular carcinoma. *Oncotarget*. 2016;7:49498-49508.
27. Bian T, Zheng L, Jiang D, et al. Overexpression of fibronectin type III domain containing 3B is correlated with epithelial-mesenchymal transition and predicts poor prognosis in lung adenocarcinoma. *Exp Ther Med*. 2019;17:3317-3326.
28. Zhong Z, Zhang H, Hong M, et al. FND3CB promotes epithelial-mesenchymal transition in tongue squamous cell carcinoma cells in a hypoxic microenvironment. *Oncol Rep*. 2018;39:1853-1859.
29. Fan X, Chen X, Deng W, Zhong G, Cai Q, Lin T. Up-regulated microRNA-143 in cancer stem cells differentiation promotes cancer cells metastasis by modulating FNDC3B expression. *BMC Cancer*. 2013;13:61.
30. Hong Y, Qin H, Li Y, et al. FND3CB circular RNA promotes the migration and invasion of gastric cancer cells via the regulation of E-cadherin and CD44 expression. *J Cell Physiol*. 2019;234:19895-19910.
31. Bondzie PA, Chen HA, Cao MZ, et al. Non-muscle myosin-IIA is critical for podocyte f-actin organization, contractility, and attenuation of cell motility. *Cytoskeleton*. 2016;73:377-395.
32. Vicente-Manzanares M, Ma X, Adelstein RS, Horwitz AR. Non-muscle myosin II takes centre stage in cell adhesion and migration. *Nat Rev Mol Cell Biol*. 2009;10:778-790.
33. Liao Q, Li R, Zhou R, et al. LIM kinase 1 interacts with myosin-9 and alpha-actinin-4 and promotes colorectal cancer progression. *Br J Cancer*. 2017;117:563-571.
34. Wang B, Qi X, Liu J, et al. MYH9 promotes growth and metastasis via activation of MAPK/AKT signaling in colorectal cancer. *J Cancer*. 2019;10:874-884.
35. Li F, Shi J, Xu Z, et al. S100A4-MYH9 axis promote migration and invasion of gastric cancer cells by inducing TGF-β-mediated epithelial-mesenchymal transition. *J Cancer*. 2018;9:3839-3849.
36. Park SY, Kim H, Yoon S, et al. KITENIN-targeting microRNA-124 suppresses colorectal cancer cell motility and tumorigenesis. *Mol Ther*. 2014;22:1653-1664.
37. Ye G, Huang K, Yu J, et al. MicroRNA-647 Targets SRF-MYH9 Axis to suppress invasion and metastasis of gastric cancer. *Theranostics*. 2017;7:3338-3353.
38. Liang S, He L, Zhao X, et al. MicroRNA let-7f inhibits tumor invasion and metastasis by targeting MYH9 in human gastric cancer. *PLoS ONE*. 2011;6:e18409.
39. Anastas JN, Moon RT. WNT signaling pathways as therapeutic targets in cancer. *Nat Rev Cancer*. 2013;13:11-26.
40. Wang W, Wen Q, Luo J, et al. Suppression of β-catenin nuclear translocation by CGP57380 decelerates poor progression and potentiates radiation-induced apoptosis in nasopharyngeal carcinoma. *Theranostics*. 2017;7:2134-2149.

How to cite this article: Li Y-Q, Chen Y, Xu Y-F, et al. *FNDC3B* 3′-UTR shortening escapes from microRNA-mediated gene repression and promotes nasopharyngeal carcinoma progression. *Cancer Sci*. 2020;111:1991–2003. https://doi.org/10.1111/cas.14394